iScience

CellPress
OPEN ACCESS

Article

# Dense residential areas promote gene flow in dengue vector mosquito *Aedes albopictus*

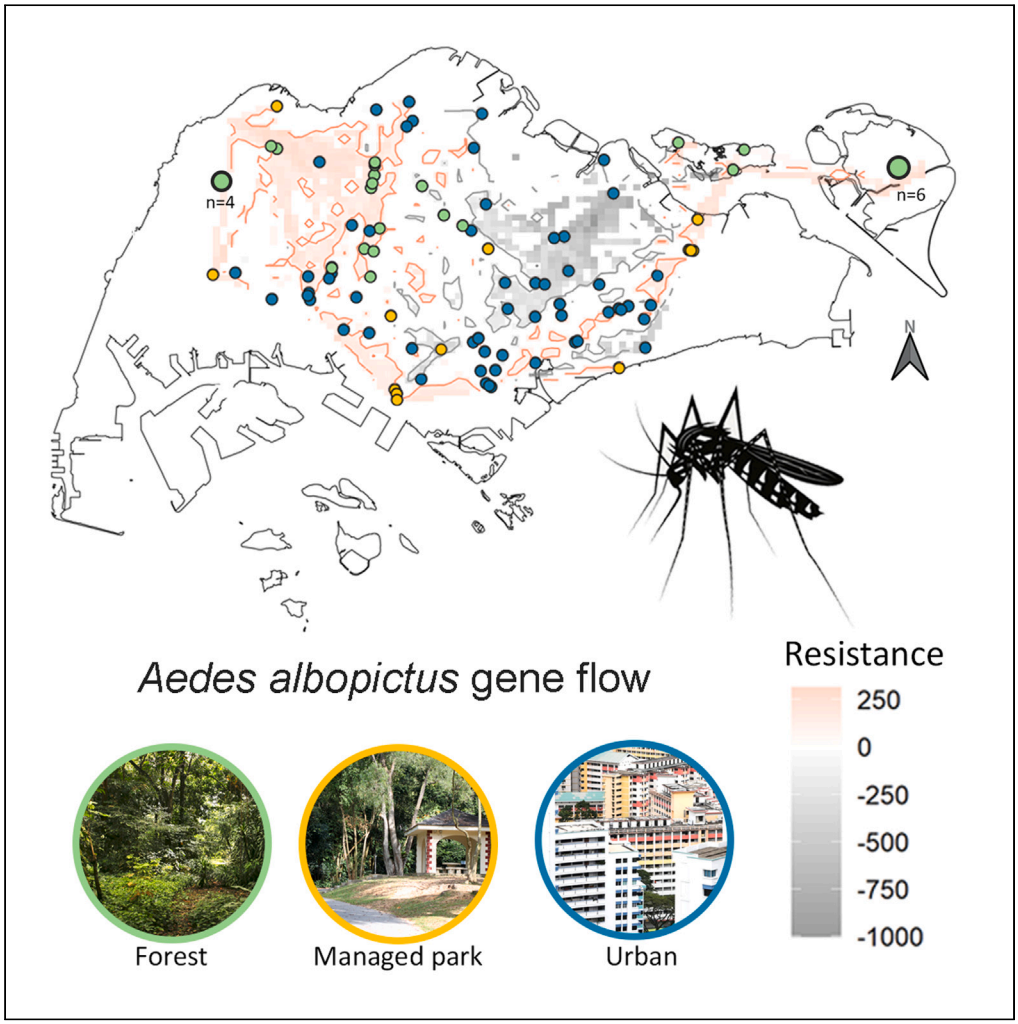


Huiqing Yeo, Hui Zhen Tan, Qian Tang, Tyrone Ren Hao Tan, Nalini Puniamoorthy, Frank E. Rheindt

huiqing_yeo@u.nus.edu (H.Y.)
nalini@nus.edu.sg (N.P.)
dbsrfe@nus.edu.sg (F.E.R.)

## Highlights

Gene flow of *Aedes albopictus* differs across habitats in a city landscape

Urban areas facilitate higher gene flow rates than parks or forests

*Wolbachia* infections of *Aedes albopictus* were characterized

Green space planning can be an ecological-based solution for vector management

Yeo et al., iScience 26, 107577
September 15, 2023 
https://doi.org/10.1016/j.isci.2023.107577

iScience

CellPress
OPEN ACCESS

Article

# Dense residential areas promote gene flow in dengue vector mosquito *Aedes albopictus*

Huiqing Yeo,[1,2,*] Hui Zhen Tan,[1] Qian Tang,[1] Tyrone Ren Hao Tan,[1] Nalini Puniamoorthy,[1,*] and Frank E. Rheindt[1,*]

## SUMMARY

***Aedes albopictus* is a successful disease vector due to its ability to survive in a wide range of habitats. Despite its ubiquity and impact on public health, little is known about its differential gene flow capabilities across different city habitats. We obtained a comprehensive dataset of >27,000 genome-wide DNA markers across 105 wild-caught *Ae. albopictus* individuals from Singapore, a dengue-endemic tropical city with heterogeneous landscapes from densely populated urban areas to forests. Despite Singapore's challenging small-scale heterogeneity, our landscape-genomic approach indicated that dense urban areas are characterized by higher *Aedes* gene flow rates than managed parks and forests. We documented the incidence of *Wolbachia* infections of *Ae. albopictus* involving two strains (*w*AlbA and *w*AlbB). Our results dispel the misconception that substantial dispersal of *Ae. albopictus* is limited to urban greenery, with wide implications for vector management and critical insights into urban planning strategies to combat dengue transmission.**

## INTRODUCTION

Dengue is a major epidemiological threat to an estimated 3.9 billion people from over 120 countries.[1] The number of dengue cases has increased 8-fold over the last two decades, with most of the disease burden (~70%) falling on countries in Asia.[2] With no specific therapeutics and no effective vaccine that can be adopted widely, dengue can be a life-threatening disease.[3] Despite substantial global vector control efforts, the rapid emergence and global spread of dengue have not been hindered.[4]

The dengue virus is mainly transmitted by *Aedes* mosquitoes in the subgenus *Stegomyia*, of which *Aedes aegypti* (Linnaeus, 1762) and *Aedes albopictus* (Skuse, 1894) are the two most common invasive disease vectors. Besides dengue, these species are also incriminated in epidemics of Zika, chikungunya, and yellow fever globally.[5] Widely considered as the primary vector for dengue virus, *Ae. aegypti* has been the subject of intensive population control in the past few decades.[6] As this vector species commonly co-occurs with *Ae. albopictus* and they engage in interspecific competition,[7,8] the ongoing eradication efforts targeting *Ae. aegypti* raise concerns that *Ae. albopictus* may take over the ecological niche of *Ae. aegypti* and become an even more efficient vector owing to its ability to adapt to a wide range of habitats.[7,9] Understanding and managing these vectors are an important public health issue especially considering that *Ae. albopictus* can be a bridge vector[10,11] and disease transmission in densely populated areas can be rapid.[12,13] Successful vector control programs rely crucially on our knowledge of gene flow dynamics and population genetic structure of vector species, including how natural landscape features and man-made structures may affect or facilitate dispersal.[14–16] Many studies have explored the invasion pathways of *Ae. albopictus* at a regional and international scale.[17–19] However, for city-specific vector control programs, fine-scale geographical data are needed to identify specific urban landscape features that facilitate or impair gene flow. This is especially so since *Ae. albopictus* is able to thrive in a wide range of natural and artificial habitats.[20]

Widely thought to have originated in forests,[10,20] *Ae. albopictus* is presently considered ecotonal and preferentially occurs in degraded and managed landscapes.[21,22] It is even found in densely populated urban areas,[20] typically characterized by little vegetation and an abundance of artificial larval breeding sources and human hosts. Despite its ubiquitous status, habitat fragmentation and various environmental stressors can disrupt gene flow and lead to the buildup of population genetic structure.[23] Certain environmental features such as human transportation networks can facilitate passive dispersal[24] or act as barriers to active dispersal.[25] Importantly, such corridors and barriers to gene flow may also impact allele frequencies that have a bearing on epidemiologically relevant traits such as vector competency[26,27] and insecticide resistance.[28,29] This in turn may affect the adaptations of *Ae. albopictus* to local conditions and can be important for its survival.

In recent years, the artificial introduction of foreign *Wolbachia* strains into various mosquito vector species has been widely employed as a sterile insect technique to control vector populations.[30,31] In Singapore, the *Wolbachia* strain *w*AlbB naturally occurring in *Ae. albopictus* is used in the control of *Ae. aegypti*.[32] Following the success of *Ae. aegypti* population suppression using *Wolbachia* technology, there are

[1]Department of Biological Sciences, National University of Singapore, 16 Science Drive 4, Singapore 117558, Singapore
[2]Lead contact
*Correspondence: huiqing_yeo@u.nus.edu (H.Y.), nalini@nus.edu.sg (N.P.), dbsrfe@nus.edu.sg (F.E.R.)
https://doi.org/10.1016/j.isci.2023.107577

increasing global concerns that niche replacement by *Ae. albopictus* can occur when *Ae. aegypti* is reduced significantly or eliminated.[32–34] Current countermeasures under consideration include the introduction of foreign *Wolbachia* strains into *Ae. albopictus* to attain the same cytoplasmic incompatibility phenotype for population suppression.[35,36] However, *Ae. albopictus* is naturally infected with multiple *Wolbachia* strains at high prevalence in the field,[37] rendering the additional introduction of a foreign *Wolbachia* strain for vector control more challenging in this species. The distribution and interaction of superinfections are not well understood but are arguably important as the success of *Wolbachia* technology hinges on our knowledge of infection loads in natural populations and how the environment may influence *Wolbachia* densities.

Different habitat types can influence *Wolbachia* infection type and densities across insects, and *Wolbachia* densities can be highly variable even across populations.[38–40] This may be a result of abiotic factors, such as differences in temperature, as well as resource availability and existing prevalent *Wolbachia* strains within a population.[41–43] Hence, it is important to characterize strains of *Wolbachia* in natural populations of *Ae. albopictus* and establish their field prevalence across heterogeneous landscapes including forests, parks, and urban areas.

In this study, we implemented an integrative approach to shed light on factors influencing gene flow in *Ae. albopictus* and shaping disease transmission dynamics in Singapore. By using a genomic technique (double-digest restriction-site-associated DNA sequencing [ddRADseq]) and employing real-time PCR, we elucidated the population structure of *Ae. albopictus* in Singapore and associated gene flow patterns with landscape features and *Wolbachia* infection status. Importantly, we show that the highest gene flow rates are concentrated in dense urban agglomerations and that urban landscape features can spur higher levels of gene flow than forests and belts of urban greenery (e.g., managed parks, streetscape). This result sheds light on the role of man-made infrastructure facilitating vector movement and disease spread in high-density urban areas.

## RESULTS

### Population genomic structure of *Aedes albopictus* in Singapore

Using a ddRADSeq protocol, more than 27,000 single-nucleotide polymorphisms (SNPs) at an average coverage of 17.3X were recovered from 107 *Ae. albopictus* individuals. After removing two individuals which were closely related to other individuals, we observed weak population structure in the remaining 105 *Ae. albopictus* sampled across Singapore, suggesting the presence of corridors and barriers to gene flow and that the population is not homogeneous.

The population in Singapore was characterized by a mean observed heterozygosity $H_O$ ($\bar{x}$ = 0.03455, SE = 0.000317) that is lower than the mean expected heterozygosity $H_e$ ($\bar{x}$ = 0.0548, SE = 0.000428), demonstrating the presence of population structure in *Ae. albopictus*. Correspondingly, the calculated inbreeding coefficient $F_{IS}$ ($\bar{x}$ = 0.369, SE = 0.00203) was positive. High genetic homogeneity notwithstanding, fine-scale population structure was detected with principal-component analysis (PCA) across a habitat cline from forest to managed parks and urban areas (Figure 1A). This gradient along PC1 is partly influenced by isolation by distance across Singapore (Partial Mantel R = 0.146, p value = 0.004). Model-based Bayesian population inference using STRUCTURE identified two main clusters (Figure S1) representing forest and urban areas with broad admixture. Demographic history reconstruction using Stairway Plot2 suggested that *Ae. albopictus* in Singapore commenced a decline in effective population size across all habitats about 3,000 years ago (Figure 1B).

### Spatial population structure of *Aedes albopictus* in Singapore

Mapping isolation-by-distance (IBD) residuals allowed us to infer that the extent of gene flow in *Ae. albopictus* differs across Singapore and underlies the weak population structure detected (Figure 2A). Significant negative IBD residuals indicated less genetic distance than expected under IBD and reflect corridors to gene flow mainly in the eastern parts of Singapore (Figure 2A; box i), corresponding with dense urban areas (Figure 2B). Conversely, significantly positive IBD residuals revealed barriers to gene flow in the northwest and southeast regions of Singapore (Figure 2A; boxes ii and iii). Regardless of whether resistance was calculated using sampled pairs within grids of 5 km, 10 km, or 20 km, high and low resistance areas remained consistent across Singapore (Figure S2).

### Landscape genetics

To find out if differential gene flow of *Ae. albopictus* across Singapore was associated with certain environmental features, seven different environmental layers (Figure S3) together with genetic data were optimized using the circuit theory resistance method. The analysis revealed that leaf area index and land surface type best explained the variation in pairwise genetic divergences based on Akaike's information criterion corrected for small/infinite sample size (AICc) (Figure S4A). These models ranked higher than the distance-only and null models, indicating that gene flow among *Ae. albopictus* is not wholly attributable to IBD. In general, areas with a high leaf area index reflected lower resistance to gene flow (Figure S5A). Similarly, when surface type was considered, unmanaged vegetated areas (forest and open greenery) were characterized by lower resistance values (Figure S5B). However, artificial infrastructure was associated with heterogeneous resistance values, with low resistance values assigned to buildings in residential areas, while higher resistance values were attributed to impervious surfaces such as roads (Figure S5A).

The goodness of fit of both models was low (average $R^2$ = 0.00635 and 0.0195 for leaf area index and land surface type, respectively) (Document S2), revealing that environmental features may not always exert the same influence on *Ae. albopictus* gene flow across highly heterogeneous environments. We highlight three key areas (Figures 2 and S5, boxes i–iii) across Singapore in the discussion section where the fine-scale effects of multiple environmental factors seemed to be at interplay.

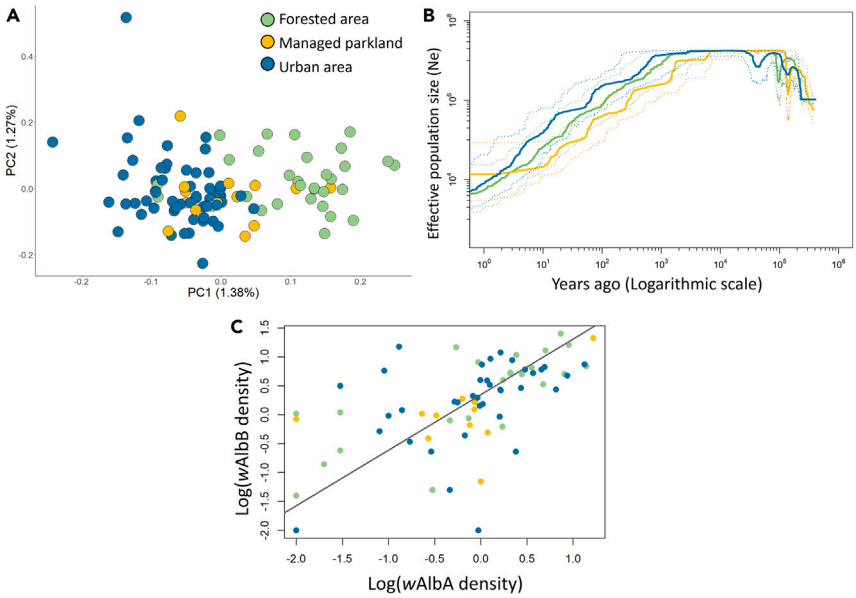


**Figure 1. Population genomic profile and *Wolbachia* incidence in *Aedes albopictus* across Singapore**

(A) Principal-component analysis (PCA) plot using 27,037 single-nucleotide polymorphisms (SNPs) showing weak clinal population structure of *Ae. albopictus* across Singapore. The percentage variation explained by each axis is shown in brackets.

(B) Demographic history of *Ae. albopictus* with decreasing effective population size over time. Solid lines indicate mean estimates of effective population size ($N_e$), and dotted lines correspond to 95% confidence intervals.

(C) Using a standardized major axis (SMA) model, *w*AlbA and *w*AlbB densities within superinfected *Ae. albopictus* individuals follow a positive correlation. p value = 3.2679e-09.

## Distribution of *Wolbachia* *w*AlbA and *w*AlbB infections in *Aedes albopictus*

A total of 77 individual *Ae. albopictus* were screened for the presence of *Wolbachia* using qPCR (26 from forest, 15 from managed parks, and 36 from urban areas). A large proportion of the *Ae. albopictus* individuals screened (85.71%) emerged as superinfected with both *w*AlbA and *w*AlbB strains (Table S1). Infection densities of *w*AlbB in *Ae. albopictus* may have differed across habitats (Kruskal-Wallis, H(2) = 6.91, p = 0.032) (Figure S6), although this pattern could have stemmed from limitations in our sampling regime. On average, *w*AlbB densities were less variable in *Ae. albopictus* from managed parks while they varied widely in mosquito individuals from forests and urban areas.

Standardized major axis (SMA) analysis was carried out to assess correlations between *w*AlbA and *w*AlbB densities within and across habitats and to test if habitat type had an interactive effect on *Wolbachia* densities of both strains. The infection densities of *w*AlbA and *w*AlbB were correlated with each other ($R^2$ = 0.379, p value = 3.2679e-09, $CI_{slope}$[0.799, 1.120], $CI_{elevation}$[0.180, 0.513]). *Ae. albopictus* individuals with higher *w*AlbA densities tended to be associated with higher *w*AlbB densities, both as a whole (Figure 1D) and within habitats (Table S2). The correlations between *w*AlbA and *w*AlbB displayed roughly the same slope and intercept among habitat types (p = 0.965), indicating that the range of correlated *Wolbachia* densities is not significantly different across habitats.

## DISCUSSION

Knowledge about mosquito dispersal is critical in the fight against dengue to untangle the dynamics of virus transmission and to design efficient control strategies. In this study, we employed an integrative approach to shed light on environmental factors and reproductive endosymbionts influencing gene flow in *Ae. albopictus* in a highly heterogeneous cityscape. In urban agglomerations, especially dense residential areas, gene flow rates of the vector species are higher than those in forests and belts of urban greenery (Figure 2). Paradoxically, areas with large highways also do not seem to promote high gene flow. This pattern indicates that while certain urban landscape features (e.g., wide roads) may not be the most conducive environments for *Ae. albopictus,* the combination of other urban features with managed vegetation (e.g., buildings and potted plants) may be responsible for high mosquito dispersal, vector movement, and disease spread in high-density urban areas.

### Barriers and corridors to gene flow at a fine geographic scale

In Singapore, urban development is often accompanied by the planting and management of greenery, creating a "city in a garden".[44] The intricate mosaic structure of this urban landscape has resulted in differential gene flow of *Ae. albopictus* even at a small geographical scale.

In the urban residential "heartland" of Singapore (Figure 2A; box i), higher-than-expected gene flow rates are associated with large contiguous urban areas (Figure 2B), possibly on account of its central location. The dispersal range of *Ae. albopictus* in urban areas may be wider than in individuals inhabiting vegetated areas. Urban areas are generally considered to be poorer quality habitats and spur larger dispersal

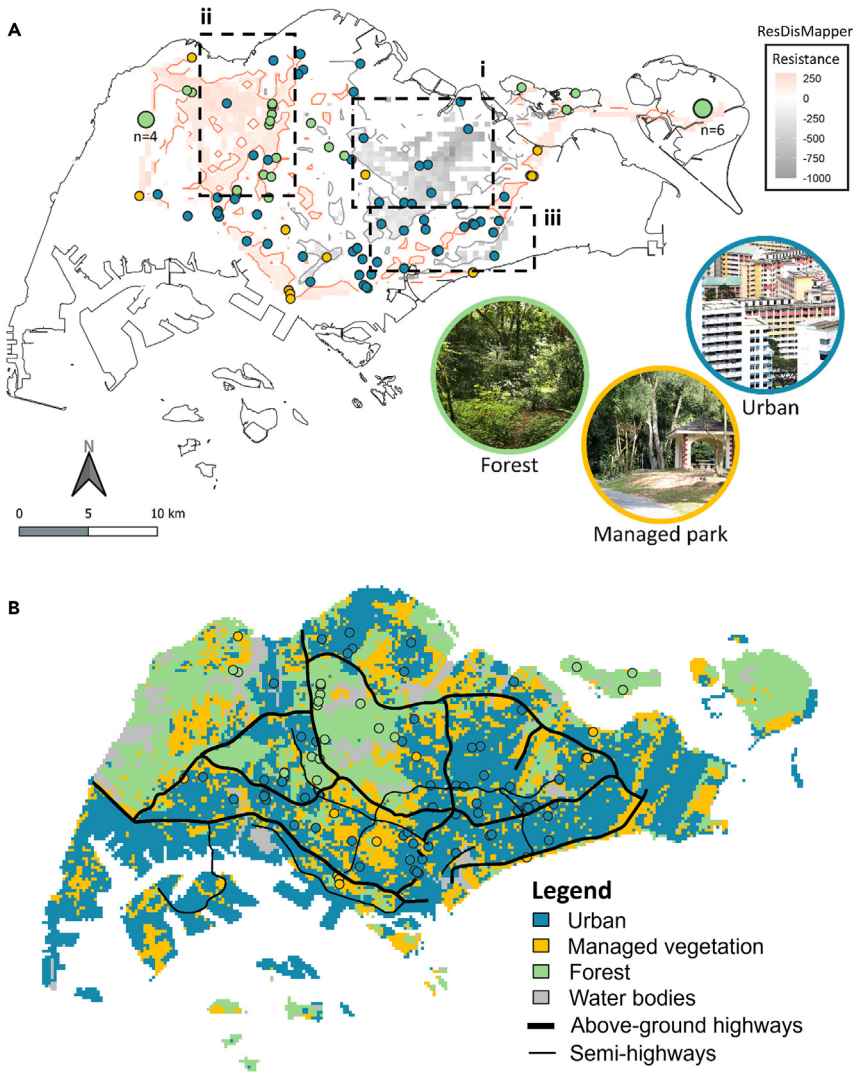


**Figure 2. Landscape heterogeneity across Singapore drives differences in *Aedes albopictus* gene flow**

(A) Sampling localities of *Ae. albopictus* overlaid with resistance values showing higher (red) or lower resistance (gray) than expected when compared to an isolation-by-distance model. Resistance values were calculated using ResDisMapper with pairs of sampled individuals within 10 km. Contour lines delineate areas statistically significant for high (red) or low (gray) resistance, respectively. Cells with no statistical certainty are not shown. Points are colored according to habitat types: forest (green), managed parks (yellow), and urban areas (blue). Boxes i, ii, and iii depict different scenarios of barriers and corridors to gene flow as discussed in the text.

(B) Habitat map of Singapore modified from Gaw et al. (2019).

distances as gravid females have to move further to seek out suitable oviposition sites, which are relatively sparse and distributed heterogeneously within the urban matrix.[45–48] The flight range, which refers to the lifetime displacement from origin, of *Ae. albopictus* is widely assumed to average around 600 m,[46,47] but individuals may also be dispersed passively through human-mediated displacement across well-connected urban areas. Additionally, pockets of greenery within the urban matrix are common in Singapore (i.e., managed vegetation under covered walkways and personal gardens of residents grown within the corridors of buildings) and can act as stepping stones in facilitating *Ae. albopictus* dispersal.

In contrast, *Ae. albopictus* individuals sampled from areas which are predominantly forested (Figure 2A, box ii) reflected lower gene flow rates. Besides targeting humans, *Ae. albopictus* feeds on a wide range of host species including dogs, pigs, and chickens.[49] As breeding habitat tends to be more homogeneous in forested areas,[50] *Ae. albopictus* populations there may experience less dispersal and hence less gene flow. Additionally, gene flow rates in the specific area we identified (Figure 2A, box ii) are likely disrupted by two highways (Bukit Timah Road and Bukit Timah Expressway). While roads have been identified to facilitate long-range passive transport of *Aedes* species likely through hitchhiking on ground vehicles,[51] they have also been reported to act as barriers to gene flow across adjacent habitats.[25]

Similarly, multiple highways in the southeast of Singapore likely contributed to the lower-than-expected gene flow rates there. A prominent area of low gene flow in this part of Singapore (Figure 2A, narrow red band in box iii) corresponds to the presence of several highways (Pan-Island Expressway and East Coast Parkway) which are nestled within the largely urban residential matrix (Figure 2B). In such areas, the landscape is additionally characterized by a high leaf area index as a result of Singapore's decades-old streetscaping efforts.[52] This practice has given rise to mature trees with ample foliage lining high-traffic highways, while the four- to eight-lane highways themselves likely constitute a barrier to gene flow in *Aedes*.[53,54]

In the same vein, urban residential areas are not fully built out with concrete and are interspersed with streetscape and indoors greenery. Such nuances in the landscape likely lead to high variability in the goodness of fit in our optimized models, highlighting the complexities of inferring drivers and barriers to gene flow in a widely distributed vector across a heterogeneous cityscape.

### Co-occurrence of *Aedes aegypti* and *Aedes albopictus*

Since the 1960s, *Ae. aegypti* has been designated the main dengue vector in Singapore.[55,56] However, internationally, an increasing number of dengue outbreaks are driven by *Ae. albopictus*,[57] which is characterized by a highly anthropogenic blood-feeding habit even at a relatively low abundance of humans.[58] Our findings support the suitability of core residential areas in Singapore for *Ae. albopictus* dispersal, including those that have historically harbored the highest number of dengue cases.[56,59,60] Against this backdrop, our results highlight that the relative importance of *Ae. aegypti* versus *Ae. albopictus* in dengue transmission remains understudied and caution that *Ae. albopictus* could potentially develop into an even more serious disease vector in Singapore and beyond.

Despite the co-occurrence of *Ae. albopictus* with urban specialist and anthropophilic *Ae. aegypti*,[56] interspecific competition does not seem to negatively impact *Ae. albopictus* gene flow in urban areas (Figure S4A). Our results highlight the highly dynamic nature of *Ae. albopictus* movement and gene flow in a heterogeneous landscape and point to a need to consider a combination of multiple environmental factors to identify key corridors and barriers in urban planning.

### Genetic connectivity of *Aedes albopictus* across Singapore

With a dataset spanning more than 27,000 genome-wide SNPs, we detected fine-scale population structure in *Ae. albopictus* across habitats (Figures 1A and S1). Part of this structure is contributed by the ubiquitous background effects of IBD (Partial Mantel R: 14.6%), which leads to a closer relationship among individuals in proximity than among those further apart. Most of the habitats with a dense forest character are distributed in the northwest and central areas of Singapore. In contrast, urban habitats are more prevalent in the southeast region, dominated by high-rise buildings with a dense human population.

### Inference of past demographic history

Stairway plot analysis suggested a decrease in effective population size of *Ae. albopictus* through time across all habitats starting around 3,000 years ago, assuming ~17 generations per year (Figure 1B). This trend persists when accounting for uncertainty in generation time: for instance, with a setting of 26 generations per year based on observations from a captive *Ae. albopictus* population in Singapore (data not shown), the continuous decrease in effective population size would have commenced more than ~1,000 years ago. While this species is thought to have originated in continental Southeast Asia,[20] the first description of *Ae. albopictus* dates to 1894 from India, and closely related species are mostly distributed across the subtropics extending from India through southern China and Japan.[61] A recent population genetic study examining *Ae. albopictus* from China, Japan, and Thailand placed the most basal *Ae. albopictus* population in China.[62] The first official record of *Ae. albopictus* in Singapore was in 1957,[63,64] and it is currently not known if the *Ae. albopictus* population in Singapore has an invasive origin. A relatively recent arrival, paired with intensive local vector control efforts in the last six decades, could potentially explain the low effective population size observed in our analysis, consistent with studies suggesting that invasive species tend to have a lower genetic diversity as a result of founder effects.[65–67]

### *Wolbachia* *w*AlbA and *w*AlbB infection loads in *Aedes albopictus* across habitats

Beyond physical landscape features, the distribution and infection load of *Ae. albopictus* with reproductive endosymbionts is crucial to understanding current patterns of mosquito prevalence and to informing control strategies. The significant positive association between *w*AlbA and *w*AlbB densities across *Ae. albopictus* individuals indicates that superinfections of both strains within a mosquito are not in antagonistic competition. Our results corroborated a previous study of *Wolbachia* density in *Ae. albopictus*,[68] strongly suggesting that *Wolbachia* superinfections interact synergistically or are independent of one another within the mosquito host.

With the growing interest to adopt novel *Wolbachia* control techniques in various *Aedes* mosquitoes, infection loads and strain interaction in mosquito hosts warrant more focus in future studies. Currently, there are only few studies employing methods to quantify *Wolbachia* infection load in wild mosquitoes.[68,69] Knowledge of *Wolbachia* strains, infection status, and strain interactions can help improve implementation of successful mosquito control programs, especially in vector species where *Wolbachia* superinfections are common.

### Limitations of the study

We have included current available landscape rasters in the landscape-genomic analyses to identify key features associated with barriers and corridors to gene flow. Geographical datasets at a finer scale can offer more accurate insights in model testing of *Ae. albopictus* gene flow

across heterogeneous landscapes, but such datasets are unfortunately not available. Even with our efforts to sample comprehensively across the city (which includes extensive terrain classified as sensitive military zones), multiple areas remain where additional sampling would have yielded a more complete dataset.

### Conclusions

The findings from this study shed light on the dispersal and invasive potential of *Ae. albopictus* and identify key landscape features associated with barriers and corridors to gene flow within a heterogeneous city matrix. Importantly, we discovered that the highest gene flow rates in *Ae. albopictus* are present in dense urban agglomerations. Surprisingly, gene flow rates of *Ae. albopictus* are lower in forests and belts of urban greenery, demonstrating that these areas are not necessarily conducive to gene flow despite the species being widely known to inhabit these areas preferentially. This conclusion has wide implications for vector management and provides useful insights into developing strategic urban planning (e.g., green space planning) to combat dengue transmission. The results of *Wolbachia* *w*AlbA and *w*AlbB infection densities, distribution, and habitat association are useful to inform future vector control projects which rely on the release of *Wolbachia*-infected *Aedes* mosquitoes and provide a baseline estimate for current *Wolbachia* superinfections in wild *Ae. albopictus*.

## STAR★METHODS

Detailed methods are provided in the online version of this paper and include the following:

- KEY RESOURCES TABLE
- RESOURCE AVAILABILITY
  - Lead contact
  - Materials availability
  - Data and code availability
- EXPERIMENTAL MODEL AND STUDY PARTICIPANT DETAILS
  - Mosquito samples
- METHOD DETAILS
  - Identification and storage
  - Extraction and library preparation
  - Demultiplexing, filtering and SNP calling
  - Quantitative PCR
- QUANTIFICATION AND STATISTICAL ANALYSIS
  - Population genomic approaches
  - Landscape genetic optimisation
  - *Wolbachia* density analyses

## SUPPLEMENTAL INFORMATION

Supplemental information can be found online at https://doi.org/10.1016/j.isci.2023.107577.

## ACKNOWLEDGMENTS

We acknowledge the National Parks Board Singapore (NP/RP18-120-2) for approval to access research sites. We thank the National Environment Agency (NEA) for approval to collect and keep mosquito samples (NEA/PH/CLB/21-00002) and for sharing samples collected by the field officers for this project (MTA-EHI-178). This work was supported by the National Centre for Infectious Diseases Catalyst Grant (FY202021NP/A-0004763-00-00) to NP and the Wildlife Reserves Singapore Conservation Fund (A-0004765-00-00) to FER.

We are grateful to C. Hapuarachchi from the Environmental Health Institute, NEA, for collaboration and input on the manuscript. We thank T.L.T. Ming and P.D.L.H. Yeong from the Military Medicine Institute, Singapore Armed Forces, for providing samples from restricted areas. Lastly, we thank members of the Avian Evolution Lab and Reproductive Evolution Lab for their assistance.

## AUTHOR CONTRIBUTIONS

Conceptualization: H.Y. and F.E.R.; Methodology, Formal Analysis, Data Curation, Validation and Visualization: H.Y.; Investigation: H.Y. and T.R.H.T.; Resources: F.E.R. and N.P.; Writing – Original Draft: H.Y.; Writing – Reviewing & Editing: F.E.R., H.Z.T., Q.T., and N.P.; Supervision: F.E.R. and N.P.; Project Administration: N.P. and F.E.R.; Funding Acquisition: N.P., F.E.R., and H.Y.

All authors read and approved the final manuscript.

## DECLARATION OF INTERESTS

The authors declare no competing interests.

## INCLUSION AND DIVERSITY

We support inclusive, diverse, and equitable conduct of research. One or more of the authors of this paper self-identifies as an underrepresented ethnic minority in their field of research or within their geographical location.

Received: February 14, 2023
Revised: May 13, 2023
Accepted: August 4, 2023
Published: August 9, 2023

## REFERENCES

1. Brady, O.J., Gething, P.W., Bhatt, S., Messina, J.P., Brownstein, J.S., Hoen, A.G., Moyes, C.L., Farlow, A.W., Scott, T.W., and Hay, S.I. (2012). Refining the global spatial limits of dengue virus transmission by evidence-based consensus. PLoS Negl. Trop. Dis. *6*, e1760. https://doi.org/10.1371/journal.pntd.0001760.
2. Bhatt, S., Gething, P.W., Brady, O.J., Messina, J.P., Farlow, A.W., Moyes, C.L., Drake, J.M., Brownstein, J.S., Hoen, A.G., Sankoh, O., et al. (2013). The global distribution and burden of dengue. Nature *496*, 504–507. https://doi.org/10.1038/nature12060.
3. Schwartz, L.M., Halloran, M.E., Durbin, A.P., and Longini, I.M. (2015). The dengue vaccine pipeline: Implications for the future of dengue control. Vaccine *33*, 3293–3298. https://doi.org/10.1016/j.vaccine.2015.05.010.
4. Gubler, D.J. (1998). Dengue and dengue hemorrhagic fever. Clin. Microbiol. Rev. *11*, 480–496. https://doi.org/10.1128/CMR.11.3.480.
5. Gratz, N.G. (2004). Critical review of the vector status of *Aedes albopictus*. Med. Vet. Entomol. *18*, 215–227. https://doi.org/10.1111/j.0269-283X.2004.00513.x.
6. World Health Organization. (2022). Dengue and Severe Dengue. https://www.who.int/news-room/fact-sheets/detail/dengue-and-severe-dengue.
7. Chan, K.L., Chan, Y.C., and Ho, B.C. (1971). *Aedes aegypti* (L.) and *Aedes albopictus* (Skuse) in Singapore City. Bull. World Health Organ. *44*, 643–649.
8. Braks, M.A.H., Honório, N.A., Lounibos, L.P., Lourenço-De-Oliveira, R., and Juliano, S.A. (2004). Interspecific competition between two invasive species of container mosquitoes, *Aedes aegypti* and *Aedes albopictus* (Diptera: Culicidae), in Brazil. Ann. Entomol. Soc. Am. *97*, 130–139. https://doi.org/10.1603/0013-8746(2004)097[0130:ICBTIS]2.0.CO;2.
9. Li, Y., Kamara, F., Zhou, G., Puthiyakunnon, S., Li, C., Liu, Y., Zhou, Y., Yao, L., Yan, G., and Chen, X.-G. (2014). Urbanization Increases *Aedes albopictus* larval habitats and accelerates mosquito development and survivorship. PLoS Negl. Trop. Dis. *8*, e3301. https://doi.org/10.1371/journal.pntd.0003301.
10. Vasilakis, N., Cardosa, J., Hanley, K.A., Holmes, E.C., and Weaver, S.C. (2011). Fever from the forest: prospects for the continued emergence of sylvatic dengue virus and its impact on public health. Nat. Rev. Microbiol. *9*, 532–541. https://doi.org/10.1038/nrmicro2595.
11. Pereira-dos-Santos, T., Roiz, D., Lourenço-de-Oliveira, R., and Paupy, C. (2020). A systematic review: Is *Aedes albopictus* an efficient bridge vector for zoonotic arboviruses? Pathogens *9*, 266. https://doi.org/10.3390/pathogens9040266.
12. Romeo-Aznar, V., Paul, R., Telle, O., and Pascual, M. (2018). Mosquito-borne transmission in urban landscapes: the missing link between vector abundance and human density. Proc. Biol. Sci. *285*, 20180826. https://doi.org/10.1098/rspb.2018.0826.
13. Kolimenakis, A., Heinz, S., Wilson, M.L., Winkler, V., Yakob, L., Michaelakis, A., Papachristos, D., Richardson, C., and Horstick, O. (2021). The role of urbanisation in the spread of *Aedes* mosquitoes and the diseases they transmit—A systematic review. PLoS Negl. Trop. Dis. *15*, e0009631. https://doi.org/10.1371/journal.pntd.0009631.
14. Schmidt, T.L., Barton, N.H., Rašić, G., Turley, A.P., Montgomery, B.L., Iturbe-Ormaetxe, I., Cook, P.E., Ryan, P.A., Ritchie, S.A., Hoffmann, A.A., et al. (2017). Local introduction and heterogeneous spatial spread of dengue-suppressing *Wolbachia* through an urban population of *Aedes aegypti*. PLoS Biol. *15*, e2001894. https://doi.org/10.1371/journal.pbio.2001894.
15. Filipović, I., Hapuarachchi, H.C., Tien, W.-P., Razak, M.A.B.A., Lee, C., Tan, C.H., Devine, G.J., and Rašić, G. (2020). Using spatial genetics to quantify mosquito dispersal for control programs. BMC Biol. *18*, 104. https://doi.org/10.1186/s12915-020-00841-0.
16. Schmidt, T.L., Endersby-Harshman, N.M., and Hoffmann, A.A. (2021). Improving mosquito control strategies with population genomics. Trends Parasitol. *37*, 907–921. https://doi.org/10.1016/j.pt.2021.05.002.
17. Kotsakiozi, P., Richardson, J.B., Pichler, V., Favia, G., Martins, A.J., Urbanelli, S., Armbruster, P.A., and Caccone, A. (2017). Population genomics of the Asian tiger mosquito, *Aedes albopictus*: insights into the recent worldwide invasion. Ecol. Evol. *7*, 10143–10157. https://doi.org/10.1002/ece3.3514.
18. Sherpa, S., Rioux, D., Pougnet-Lagarde, C., and Després, L. (2018). Genetic diversity and distribution differ between long-established and recently introduced populations in the invasive mosquito *Aedes albopictus*. Infect. Genet. Evol. *58*, 145–156. https://doi.org/10.1016/j.meegid.2017.12.018.
19. Schmidt, T.L., Chung, J., Honnen, A.-C., Weeks, A.R., and Hoffmann, A.A. (2020). Population genomics of two invasive mosquitoes (*Aedes aegypti* and *Aedes albopictus*) from the Indo-Pacific. PLoS Negl. Trop. Dis. *14*, e0008463. https://doi.org/10.1371/journal.pntd.0008463.
20. Paupy, C., Delatte, H., Bagny, L., Corbel, V., and Fontenille, D. (2009). *Aedes albopictus*, an arbovirus vector: From the darkness to the light. Microbes Infect. *11*, 1177–1185. https://doi.org/10.1016/j.micinf.2009.05.005.
21. Reiskind, M.H., Griffin, R.H., Janairo, M.S., and Hopperstad, K.A. (2017). Mosquitoes of field and forest: the scale of habitat segregation in a diverse mosquito assemblage. Med. Vet. Entomol. *31*, 44–54. https://doi.org/10.1111/mve.12193.
22. Hendy, A., Hernandez-Acosta, E., Chaves, B.A., Fé, N.F., Valério, D., Mendonça, C., Lacerda, M.V.G.d., Buenemann, M., Vasilakis, N., and Hanley, K.A. (2020). Into the woods: Changes in mosquito community composition and presence of key vectors at increasing distances from the urban edge in urban forest parks in Manaus, Brazil. Acta Trop. *206*, 105441. https://doi.org/10.1016/j.actatropica.2020.105441.
23. Watanabe, K., Monaghan, M.T., Takemon, Y., and Omura, T. (2010). Dispersal ability determines the genetic effects of habitat fragmentation in three species of aquatic insect. Aquat. Conserv. *20*, 574–579. https://doi.org/10.1002/aqc.1124.
24. Schmidt, T.L., Rašić, G., Zhang, D., Zheng, X., Xi, Z., and Hoffmann, A.A. (2017). Genome-wide SNPs reveal the drivers of gene flow in an urban population of the Asian Tiger Mosquito, *Aedes albopictus*. PLoS Negl. Trop. Dis. *11*, e0006009. https://doi.org/10.1371/journal.pntd.0006009.
25. Regilme, M.A.F., Carvajal, T.M., Honnen, A.-C., Amalin, D.M., and Watanabe, K. (2021). The influence of roads on the fine-scale population genetic structure of the dengue vector *Aedes aegypti* (Linnaeus). PLoS Negl. Trop. Dis. *15*, e0009139. https://doi.org/10.1371/journal.pntd.0009139.
26. Lozano-Fuentes, S., Fernandez-Salas, I., de Lourdes Munoz, M., Garcia-Rejon, J., Olson, K.E., Beaty, B.J., and Black, W.C., 4th (2009). The neovolcanic axis is a barrier to gene flow among *Aedes aegypti* populations in Mexico that differ in vector competence for dengue 2 virus. PLoS Negl. Trop. Dis. *3*, e468. https://doi.org/10.1371/journal.pntd.0000468.
27. Garcia-Luna, S.M., Weger-Lucarelli, J., Rückert, C., Murrieta, R.A., Young, M.C., Byas, A.D., Fauver, J.R., Perera, R., Flores-Suarez, A.E., Ponce-Garcia, G., et al. (2018). Variation in competence for ZIKV transmission by *Aedes aegypti* and *Aedes albopictus* in Mexico. PLoS Negl. Trop. Dis. *12*, e0006599. https://doi.org/10.1371/journal.pntd.0006599.
28. García, G.P., Flores, A.E., Fernández-Salas, I., Saavedra-Rodríguez, K., Reyes-Solis, G., Lozano-Fuentes, S., Guillermo Bond, J.,

Casas-Martínez, M., Ramsey, J.M., García-Rejón, J., et al. (2009). Recent rapid rise of a permethrin knock down resistance allele in *Aedes aegypti* in México. PLoS Negl. Trop. Dis. *3*, e531. https://doi.org/10.1371/journal.pntd.0000531.

29. Barnes, K.G., Irving, H., Chiumia, M., Mzilahowa, T., Coleman, M., Hemingway, J., and Wondji, C.S. (2017). Restriction to gene flow is associated with changes in the molecular basis of pyrethroid resistance in the malaria vector *Anopheles funestus*. Proc. Natl. Acad. Sci. *114*, 286–291. https://doi.org/10.1073/pnas.1615458114.
30. Mains, J.W., Brelsfoard, C.L., Rose, R.I., and Dobson, S.L. (2016). Female adult *Aedes albopictus* suppression by *Wolbachia*-infected male mosquitoes. Sci. Rep. *6*, 33846. https://doi.org/10.1038/srep33846.
31. Crawford, J.E., Clarke, D.W., Criswell, V., Desnoyer, M., Cornel, D., Deegan, B., Gong, K., Hopkins, K.C., Howell, P., Hyde, J.S., et al. (2020). Efficient production of male *Wolbachia*-infected *Aedes aegypti* mosquitoes enables large-scale suppression of wild populations. Nat. Biotechnol. *38*, 482–492. https://doi.org/10.1038/s41587-020-0471-x.
32. National Environment Agency (2016). Risk Assessment for the Use of Male *Wolbachia*-Carrying *Aedes aegypti* for Suppression of the *Aedes aegypti* Mosquito Population (National Environment Agency).
33. Lounibos, L.P. (2007). Competitive displacement and reduction. J. Am. Mosq. Control Assoc. *23*, 276–282.
34. Marina, C.F., Bond, J.G., Hernández-Arriaga, K., Valle, J., Ulloa, A., Fernández-Salas, I., Carvalho, D.O., Bourtzis, K., Dor, A., Williams, T., and Liedo, P. (2021). Population Dynamics of *Aedes aegypti* and *Aedes albopictus* in two rural villages in southern Mexico: Baseline data for an evaluation of the sterile insect technique. Insects *12*, 58. https://doi.org/10.3390/insects12010058.
35. Moretti, R., and Calvitti, M. (2013). Male mating performance and cytoplasmic incompatibility in a *w*Pip *Wolbachia* trans-infected line of *Aedes albopictus* (Stegomyia albopicta). Med. Vet. Entomol. *27*, 377–386. https://doi.org/10.1111/j.1365-2915.2012.01061.x.
36. Ant, T.H., and Sinkins, S.P. (2018). A *Wolbachia* triple-strain infection generates self-incompatibility in *Aedes albopictus* and transmission instability in *Aedes aegypti*. Parasit. Vectors *11*, 295. https://doi.org/10.1186/s13071-018-2870-0.
37. Zhou, W., Rousset, F., and O'Neill, S. (1998). Phylogeny and PCR–based classification of *Wolbachia* strains using wsp gene sequences. Proc. Biol. Sci. *265*, 509–515. https://doi.org/10.1098/rspb.1998.0324.
38. Hancock, P.A., White, V.L., Callahan, A.G., Godfray, C.H.J., Hoffmann, A.A., and Ritchie, S.A. (2016). Density-dependent population dynamics in *Aedes aegypti* slow the spread of wMel *Wolbachia*. J. Appl. Ecol. *53*, 785–793. https://doi.org/10.1111/1365-2664.12620.
39. Unckless, R.L., Boelio, L.M., Herren, J.K., and Jaenike, J. (2009). *Wolbachia* as populations within individual insects: causes and consequences of density variation in natural populations. Proc. Biol. Sci. *276*, 2805–2811. https://doi.org/10.1098/rspb.2009.0287.
40. Wiwatanaratanabutr, S., and Kittayapong, P. (2006). Effects of temephos and temperature on *Wolbachia* load and life history traits of *Aedes albopictus*. Med. Vet. Entomol. *20*, 300–307. https://doi.org/10.1111/j.1365-2915.2006.00640.x.
41. Dutton, T.J., and Sinkins, S.P. (2004). Strain-specific quantification of *Wolbachia* density in *Aedes albopictus* and effects of larval rearing conditions. Insect Mol. Biol. *13*, 317–322. https://doi.org/10.1111/j.0962-1075.2004.00490.x.
42. Joanne, S., Vythilingam, I., Yugavathy, N., Leong, C.-S., Wong, M.-L., and AbuBakar, S. (2015). Distribution and dynamics of *Wolbachia* infection in Malaysian *Aedes albopictus*. Acta Trop. *148*, 38–45. https://doi.org/10.1016/j.actatropica.2015.04.003.
43. Versace, E., Nolte, V., Pandey, R.V., Tobler, R., and Schlötterer, C. (2014). Experimental evolution reveals habitat-specific fitness dynamics among <i>Wolbachia<i> clades in *Drosophila melanogaster*. Mol. Ecol. *23*, 802–814. https://doi.org/10.1111/mec.12643.
44. Civil Service College. (2018). A City in a Garden. CSC.. https://www.csc.gov.sg/articles/a-city-in-a-garden.
45. Edman, J.D., Scott, T.W., Costero, A., Morrison, A.C., Harrington, L.C., and Clark, G.G. (1998). *Aedes aegypti* (Diptera: Culicidae) movement influenced by availability of oviposition sites. J. Med. Entomol. *35*, 578–583. https://doi.org/10.1093/jmedent/35.4.578.
46. Liew, C., and Curtis, C.F. (2004). Horizontal and vertical dispersal of dengue vector mosquitoes, *Aedes aegypti* and *Aedes albopictus*, in Singapore. Med. Vet. Entomol. *18*, 351–360. https://doi.org/10.1111/j.0269-283X.2004.00517.x.
47. Maciel-de-freitas, R., Neto, R.B., Gonçalves, J.M., Codeço, C.T., and Lourenço-de-Oliveira, R. (2006). Movement of dengue vectors between the human modified environment and an urban forest in Rio de Janeiro. J. Med. Entomol. *43*, 1112–1120. https://doi.org/10.1093/jmedent/43.6.1112.
48. David, M.R., Lourenço-de-Oliveira, R., and Freitas, R.M.d. (2009). Container productivity, daily survival rates and dispersal of *Aedes aegypti* mosquitoes in a high income dengue epidemic neighbourhood of Rio de Janeiro: presumed influence of differential urban structure on mosquito biology. Mem. Inst. Oswaldo Cruz *104*, 927–932. https://doi.org/10.1590/S0074-02762009000600019.
49. Fikrig, K., and Harrington, L.C. (2021). Understanding and interpreting mosquito blood feeding studies: the case of *Aedes albopictus*. Trends Parasitol. *37*, 959–975. https://doi.org/10.1016/j.pt.2021.07.013.
50. Muhammad, N.A.F., Abu Kassim, N.F., Ab Majid, A.H., Abd Rahman, A., Dieng, H., and Avicor, S.W. (2020). Biting rhythm and demographic attributes of *Aedes albopictus* (Skuse) females from different urbanized settings in Penang Island, Malaysia under uncontrolled laboratory conditions. PLoS One *15*, e0241688. https://doi.org/10.1371/journal.pone.0241688.
51. Ibáñez-Justicia, A. (2020). Pathways for introduction and dispersal of invasive *Aedes* mosquito species in Europe: A review. J. Eur. Mosq. Control Assoc. *38*, 1–10.
52. Tan, P.Y., Wang, J., and Sia, A. (2013). Perspectives on five decades of the urban greening of Singapore. Cities *32*, 24–32. https://doi.org/10.1016/j.cities.2013.02.001.
53. Russell, R.C., Webb, C.E., Williams, C.R., and Ritchie, S.A. (2005). Mark–release–recapture study to measure dispersal of the mosquito *Aedes aegypti* in Cairns, Queensland, Australia. Med. Vet. Entomol. *19*, 451–457. https://doi.org/10.1111/j.1365-2915.2005.00589.x.
54. Hemme, R.R., Thomas, C.L., Chadee, D.D., and Severson, D.W. (2010). Influence of urban landscapes on population dynamics in a short-distance migrant mosquito: evidence for the dengue vector *Aedes aegypti*. PLoS Negl. Trop. Dis. *4*, e634. https://doi.org/10.1371/journal.pntd.0000634.
55. Chan, Y.C., Chan, K.L., and Ho, B.C. (1971). *Aedes aegypti* (L.) and *Aedes albopictus* (Skuse) in Singapore city. 1. Distribution and density. Bull. World Health Organ. *44*, 617–627.
56. Ong, J., Liu, X., Rajarethinam, J., Yap, G., Ho, D., and Ng, L.C. (2019). A novel entomological index, *Aedes aegypti* Breeding Percentage, reveals the geographical spread of the dengue vector in Singapore and serves as a spatial risk indicator for dengue. Parasit. Vectors *12*, 17. https://doi.org/10.1186/s13071-018-3281-y.
57. Lambrechts, L., Scott, T.W., and Gubler, D.J. (2010). Consequences of the expanding global distribution of *Aedes albopictus* for dengue virus transmission. PLoS Negl. Trop. Dis. *4*, e646. https://doi.org/10.1371/journal.pntd.0000646.
58. Kek, R., Hapuarachchi, H.C., Chung, C.-Y., Humaidi, M.B., Razak, M.A.B.A., Chiang, S., Lee, C., Tan, C.-H., Yap, G., Chong, C.-S., et al. (2014). Feeding host range of *Aedes albopictus* (Diptera: Culicidae) demonstrates its opportunistic host-seeking behavior in rural Singapore. J. Med. Entomol. *51*, 880–884. https://doi.org/10.1603/ME13213.
59. Koou, S.-Y., Chong, C.-S., Vythilingam, I., Lee, C.-Y., and Ng, L.-C. (2014). Insecticide resistance and its underlying mechanisms in field populations of *Aedes aegypti* adults (Diptera: Culicidae) in Singapore. Parasit. Vectors *7*, 471. https://doi.org/10.1186/s13071-014-0471-0.
60. Elangovan, N. (2020). Explainer: Why Singapore's East and North Tend to Suffer the Largest Dengue Clusters Every Year. TODAY. https://www.todayonline.com/singapore/explainer-why-eastern-and-northern-parts-singapore-suffer-largest-dengue-clusters-every.
61. Mogi, M., Armbruster, P.A., Tuno, N., Aranda, C., and Yong, H.S. (2017). The climate range expansion of *Aedes albopictus* (Diptera: Culicidae) in Asia inferred from the distribution of *albopictus* subgroup species of *Aedes* (*Stegomyia*). J. Med. Entomol. *54*, 1615–1625. https://doi.org/10.1093/jme/tjx156.
62. Manni, M., Guglielmino, C.R., Scolari, F., Vega-Rúa, A., Failloux, A.-B., Somboon, P., Lisa, A., Savini, G., Bonizzoni, M., Gomulski, L.M., et al. (2017). Genetic evidence for a worldwide chaotic dispersion pattern of the arbovirus vector, *Aedes albopictus*. PLoS Negl. Trop. Dis. *11*, e0005332. https://doi.org/10.1371/journal.pntd.0005332.
63. Colless, D.H. (1957). Notes on the culicine mosquitoes of Singapore. III. Larval breeding-places. Ann. Trop. Med. Parasitol. *51*, 102–116. https://doi.org/10.1080/00034983.1957.11685799.
64. Lam-Phua, S.-G., Yeo, H., Lee, R.M.-L., Chong, C.-S., Png, A.-B., Foo, S.-Y., Liew, C., Ng, L.-C., Tang, C.-S., Rueda, L.M., et al.

(2019). Mosquitoes (Diptera: Culicidae) of Singapore: Updated checklist and new records. J. Med. Entomol. *56*, 103–119. https://doi.org/10.1093/jme/tjy154.

65. Barrett, S.C.H., and Kohn, J.R. (1991). Genetic and Evolutionary Consequences of Small Population Size in Plants: Implications for Conservation. Oxford University Press.
66. Sakai, A.K., Allendorf, F.W., Holt, J.S., Lodge, D.M., Molofsky, J., With, K.A., Baughman, S., Cabin, R.J., Cohen, J.E., Ellstrand, N.C., et al. (2001). The population biology of invasive species. Annu. Rev. Ecol. Syst. *32*, 305–332.
67. Hawley, D.M., Hanley, D., Dhondt, A.A., and Lovette, I.J. (2006). Molecular evidence for a founder effect in invasive house finch (Carpodacus mexicanus) populations experiencing an emergent disease epidemic. Mol. Ecol. *15*, 263–275. https://doi.org/10.1111/j.1365-294X.2005.02767.x.
68. Yang, Q., Chung, J., Robinson, K.L., Schmidt, T.L., Ross, P.A., Liang, J., and Hoffmann, A.A. (2022). Sex-specific distribution and classification of *Wolbachia* infections and mitochondrial DNA haplogroups in *Aedes albopictus* from the Indo-Pacific. PLoS Negl. Trop. Dis. *16*, e0010139. https://doi.org/10.1101/2022.01.05.475177.
69. Ahantarig, A., Trinachartvanit, W., and Kittayapong, P. (2008). Relative *Wolbachia* density of field-collected *Aedes albopictus* mosquitoes in Thailand. J. Vector Ecol. *33*, 173–177. https://doi.org/10.3376/1081-1710(2008)33[173:RWDOFA]2.0.CO;2.
70. Hu, Y., Xi, Z., Liu, X., Wang, J., Guo, Y., Ren, D., Wu, H., Wang, X., Chen, B., and Liu, Q. (2020). Identification and molecular characterization of *Wolbachia* strains in natural populations of *Aedes albopictus* in China. Parasit. Vectors *13*, 28. https://doi.org/10.1186/s13071-020-3899-4.
71. Martin, M. (2011). Cutadapt removes adapter sequences from high-throughput sequencing reads. EMBnet. j. *17*, 10–12. https://doi.org/10.14806/ej.17.1.200.
72. Wingett, S.W., and Andrews, S. (2018). FastQ Screen: a tool for multi-genome mapping and quality control. F1000Res. *7*, 1338. https://doi.org/10.12688/f1000research.15931.2.
73. Catchen, J.M., Amores, A., Hohenlohe, P., Cresko, W., and Postlethwait, J.H. (2011). Stacks: Building and genotyping loci *de novo* from short-read sequences. G3 (Bethesda) *1*, 171–182. https://doi.org/10.1534/g3.111.000240.
74. Li, H. (2013). Aligning sequence reads, clone sequences and assembly contigs with BWA-MEM. Preprint at arXiv. http://arxiv.org/abs/1303.3997.
75. Li, H., Handsaker, B., Wysoker, A., Fennell, T., Ruan, J., Homer, N., Marth, G., Abecasis, G., and Durbin, R.; 1000 Genome Project Data Processing Subgroup (2009). Genome Project Data Processing Subgroup (2009). The Sequence Alignment/Map format and SAMtools. Bioinformatics *25*, 2078–2079. https://doi.org/10.1093/bioinformatics/btp352.
76. Alexander, D.H., Novembre, J., and Lange, K. (2009). Fast model-based estimation of ancestry in unrelated individuals. Genome Res. *19*, 1655–1664. https://doi.org/10.1101/gr.094052.109.
77. Purcell, S., Neale, B., Todd-Brown, K., Thomas, L., Ferreira, M.A.R., Bender, D., Maller, J., Sklar, P., de Bakker, P.I.W., Daly, M.J., and Sham, P.C. (2007). PLINK: A tool set for whole-genome association and population-based linkage analyses. Am. J. Hum. Genet. *81*, 559–575. https://doi.org/10.1086/519795.
78. Pritchard, J.K., Stephens, M., and Donnelly, P. (2000). Inference of population structure using multilocus genotype data. Genetics *155*, 945–959. https://doi.org/10.1093/genetics/155.2.945.
79. Lischer, H.E.L., and Excoffier, L. (2012). PGDSpider: an automated data conversion tool for connecting population genetics and genomics programs. Bioinformatics *28*, 298–299. https://doi.org/10.1093/bioinformatics/btr642.
80. Korneliussen, T.S., Albrechtsen, A., and Nielsen, R. (2014). ANGSD: Analysis of Next Generation Sequencing Data. BMC Bioinf. *15*, 356. https://doi.org/10.1186/s12859-014-0356-4.
81. Liu, X., and Fu, Y.-X. (2020). Stairway Plot 2: demographic history inference with folded SNP frequency spectra. Genome Biol. *21*, 280. https://doi.org/10.1186/s13059-020-02196-9.
82. R Core Team (2022). R: A Language and Environment for Statistical Computing (Vienna, Austria: R Foundation for Statistical Computing). https://www.R-project.org/.
83. Pfeifer, B., Wittelsbürger, U., Ramos-Onsins, S.E., and Lercher, M.J. (2014). PopGenome: An efficient swiss army knife for population genomic analyses in R. Mol. Biol. Evol. *31*, 1929–1936. https://doi.org/10.1093/molbev/msu136.
84. Goudet, J. (2005). hierfstat, a package for r to compute and test hierarchical F-statistics. Mol. Ecol. Notes *5*, 184–186. https://doi.org/10.1111/j.1471-8286.2004.00828.x.
85. Zheng, X., Levine, D., Shen, J., Gogarten, S.M., Laurie, C., and Weir, B.S. (2012). A high-performance computing toolset for relatedness and principal component analysis of SNP data. Bioinformatics *28*, 3326–3328. https://doi.org/10.1093/bioinformatics/bts606.
86. Bjornstad, O.N. (2020). Ncf Spat. Covariance Funct. R Package Version 12-9. https://CRAN.R-project.org/package=ncf.
87. Kamvar, Z.N., Tabima, J.F., and Grünwald, N.J. (2014). Poppr: an R package for genetic analysis of populations with clonal, partially clonal, and/or sexual reproduction. PeerJ *2*, e281. https://doi.org/10.7717/peerj.281.
88. Tang, Q., Fung, T., and Rheindt, F.E. (2020). ResDisMapper: An R package for fine-scale mapping of resistance to dispersal. Mol. Ecol. Resour. *20*, 819–831. https://doi.org/10.1111/1755-0998.13127.
89. Peterman, W.E. (2018). ResistanceGA: An R package for the optimization of resistance surfaces using genetic algorithms. Methods Ecol. Evol. *9*, 1638–1647. https://doi.org/10.1111/2041-210X.12984.
90. Warton, D.I., Duursma, R.A., Falster, D.S., and Taskinen, S. (2012). SMATR 3 - an R package for estimation and inference about allometric lines. Methods Ecol. Evol. *3*, 257–259. https://doi.org/10.1111/j.2041-210X.2011.00153.x.
91. Meteorological Service Singapore (2022). Climate of Singapore. Clim. Singap. http://www.weather.gov.sg/climate-climate-of-singapore/.
92. Gaw, L.Y.-F., Yee, A.T.K., and Richards, D.R. (2019). A high-resolution map of Singapore's terrestrial ecosystems. Data *4*, 116. https://doi.org/10.3390/data4030116.
93. Li, Y., Su, X., Zhou, G., Zhang, H., Puthiyakunnon, S., Shuai, S., Cai, S., Gu, J., Zhou, X., Yan, G., and Chen, X.G. (2016). Comparative evaluation of the efficiency of the BG-Sentinel trap, CDC light trap and mosquito-oviposition trap for the surveillance of vector mosquitoes. Parasit. Vectors *9*, 446. https://doi.org/10.1186/s13071-016-1724-x.
94. Gorsich, E.E., Beechler, B.R., van Bodegom, P.M., Govender, D., Guarido, M.M., Venter, M., and Schrama, M. (2019). A comparative assessment of adult mosquito trapping methods to estimate spatial patterns of abundance and community composition in southern Africa. Parasit. Vectors *12*, 462. https://doi.org/10.1186/s13071-019-3733-z.
95. Peterson, B.K., Weber, J.N., Kay, E.H., Fisher, H.S., and Hoekstra, H.E. (2012). Double digest RADseq: An inexpensive method for *de novo* SNP discovery and genotyping in model and non-model species. PLoS One *7*, e37135. https://doi.org/10.1371/journal.pone.0037135.
96. Tang, Q., Shingate, P., Wardiatno, Y., John, A., Tay, B.H., Tay, Y.C., Yap, L.-M., Lim, J., Tong, H.Y., Tun, K., et al. (2021). The different fates of two Asian horseshoe crab species with different dispersal abilities. Evol. Appl. *14*, 2124–2133. https://doi.org/10.1111/eva.13271.
97. Catchen, J., Hohenlohe, P.A., Bassham, S., Amores, A., and Cresko, W.A. (2013). Stacks: An analysis tool set for population genomics. Mol. Ecol. *22*, 3124–3140. https://doi.org/10.1111/mec.12354.
98. Palatini, U., Masri, R.A., Cosme, L.V., Koren, S., Thibaud-Nissen, F., Biedler, J.K., Krsticevic, F., Johnston, J.S., Halbach, R., Crawford, J.E., et al. (2020). Improved reference genome of the arboviral vector *Aedes albopictus*. Genome Biol. *21*, 215. https://doi.org/10.1186/s13059-020-02141-w.
99. Alexander, D.H., and Lange, K. (2011). Enhancements to the ADMIXTURE algorithm for individual ancestry estimation. BMC Bioinf. *12*, 246. https://doi.org/10.1186/1471-2105-12-246.
100. De la Cruz, O., and Raska, P. (2014). Population structure at different minor allele frequency levels. BMC Proc. *8*, S55. https://doi.org/10.1186/1753-6561-8-S1-S55.
101. Chang, C.C., Chow, C.C., Tellier, L.C., Vattikuti, S., Purcell, S.M., and Lee, J.J. (2015). Second-generation PLINK: rising to the challenge of larger and richer datasets. GigaScience *4*, 7. https://doi.org/10.1186/s13742-015-0047-8.
102. Nielsen, R., Paul, J.S., Albrechtsen, A., and Song, Y.S. (2011). Genotype and SNP calling from next-generation sequencing data. Nat. Rev. Genet. *12*, 443–451. https://doi.org/10.1038/nrg2986.
103. Schmidt, T.L., Jasper, M.-E., Weeks, A.R., and Hoffmann, A.A. (2021). Unbiased population heterozygosity estimates from genome-wide sequence data. Methods Ecol. Evol. *12*, 1888–1898. https://doi.org/10.1111/2041-210X.13659.
104. Milligan, B.G. (2003). Maximum-likelihood estimation of relatedness. Genetics *163*, 1153–1167. https://doi.org/10.1093/genetics/163.3.1153.
105. Choi, Y., Wijsman, E.M., and Weir, B.S. (2009). Case-control association testing in the presence of unknown relationships. Genet. Epidemiol. *33*, 668–678. https://doi.org/10.1002/gepi.20418.

106. Pina-Martins, F., Silva, D.N., Fino, J., and Paulo, O.S. (2017). Structure_threader: An improved method for automation and parallelization of programs structure, fastStructure and MavericK on multicore CPU systems. Mol. Ecol. Resour. *17*, e268–e274. https://doi.org/10.1111/1755-0998.12702.

107. Evanno, G., Regnaut, S., and Goudet, J. (2005). Detecting the number of clusters of individuals using the software structure: a simulation study. Mol. Ecol. *14*, 2611–2620. https://doi.org/10.1111/j.1365-294X.2005.02553.x.

108. Earl, D.A., and vonHoldt, B.M. (2012). STRUCTURE HARVESTER: A website and program for visualizing STRUCTURE output and implementing the Evanno method. Conserv. Genet. Resour. *4*, 359–361. https://doi.org/10.1007/s12686-011-9548-7.

109. Jakobsson, M., and Rosenberg, N.A. (2007). CLUMPP: A cluster matching and permutation program for dealing with label switching and multimodality in analysis of population structure. Bioinformatics *23*, 1801–1806. https://doi.org/10.1093/bioinformatics/btm233.

110. Keightley, P.D., Ness, R.W., Halligan, D.L., and Haddrill, P.R. (2014). Estimation of the spontaneous mutation rate per nucleotide site in a *Drosophila melanogaster* full-sib family. Genetics *196*, 313–320. https://doi.org/10.1534/genetics.113.158758.

111. Rašić, G., Filipović, I., Weeks, A.R., and Hoffmann, A.A. (2014). Genome-wide SNPs lead to strong signals of geographic structure and relatedness patterns in the major arbovirus vector, *Aedes aegypti*. BMC Genom. *15*, 275. https://doi.org/10.1186/1471-2164-15-275.

112. Chan, K.L. (1971). Life table studies of *Aedes albopictus* (Skuse). In Sterility principle for insect control or eradication (International Atomic Energy Agency)), pp. 131–143.

113. McRae, B.H., Dickson, B.G., Keitt, T.H., and Shah, V.B. (2008). Using circuit theory to model connectivity in ecology, evolution, and conservation. Ecology *89*, 2712–2724. https://doi.org/10.1890/07-1861.1.

114. Van Strien, M.J., Keller, D., and Holderegger, R. (2012). A new analytical approach to landscape genetic modelling: least-cost transect analysis and linear mixed models. Mol. Ecol. *21*, 4010–4023. https://doi.org/10.1111/j.1365-294X.2012.05687.x.

115. Akaike, H. (1974). A new look at the statistical model identification. IEEE Trans. Automat. Contr. *19*, 716–723. https://doi.org/10.1109/TAC.1974.1100705.

116. (2022). Urban redevelopment authority master plan 2019 land use layer. Data.gov.sg. https://data.gov.sg/dataset/master-plan-2019-land-use-layer.

117. National Environment Agency (2021). Dengue clusters. Data.gov.sg. https://data.gov.sg/dataset/dengue-clusters.

118. National Environment Agency (2018). Dengue Cases. Data.gov.Sg. https://data.gov.sg/dataset/dengue-cases.

119. National Environment Agency (2021). Areas with High Aedes Population. Data.gov.Sg. https://data.gov.sg/dataset/areas-with-high-aedes-population.

120. Richards, D., and Wang, J.W. (2020). Fusing street level photographs and satellite remote sensing to map leaf area index. Ecol. Indic. *115*, 106342. https://doi.org/10.1016/j.ecolind.2020.106342.

## STAR★METHODS

### KEY RESOURCES TABLE

| REAGENT or RESOURCE | SOURCE | IDENTIFIER |
|---|---|---|
| Chemicals, peptides, and recombinant proteins | | |
| Enzyme EcoRI | BioLabs | R0101S |
| Enzyme MspI | BioLabs | R0106S |
| NEB CutSmart buffer | BioLabs | B6004 |
| T4 DNA ligase | BioLabs | M0202L |
| Ampure XP paramagnetic beads | Beckman Coulter | A63880 |
| Pippin prep 2% gel cassette, external markers | Sage Sciences | CEF2010 |
| Critical commercial assays | | |
| DNeasy Blood & Tissue Kit | Qiagen | 69506 |
| NEBNext® Multiplex Oligos for Illumina® | BioLabs | E7600S |
| Qubit™ dsDNA HS Assay Kit | Invotrogen | Q32854 |
| SsoAdvancedTM Universal SYBR® Green Supermix | Bio-Rad | 1725270 |
| Q5 Hot Start High-Fidelity DNA polymerase and buffer | BioLabs | M0493S |
| Deposited data | | |
| Raw sequence data | This paper, GenBank | BioProject number: PRJNA988429 |
| Sample metadata | This paper, Mendeley Data | https://data.mendeley.com/datasets/tsf62dsvd4/1 |
| Code | This paper, Github | https://github.com/huiqingyeooo/Ae_albopictus_popgen |
| Oligonucleotides | | |
| Primers for *Wolbachia* wAlbA and wAlbB detection, see Table S4 | Hu et al.[70] | N/A |
| Primers for *Aedes* housekeeping gene, see Table S4 | Dutton and Sinkins[41] | N/A |
| Software and algorithms | | |
| CutAdapt | Martin[71] | https://journal.embnet.org/index.php/embnetjournal/article/view/200 |
| FastQC | Babraham Bioinformatics[72] | https://www.bioinformatics.babraham.ac.uk/projects/fastqc/ |
| Stacks v2.41 | Catchen et al.[73] | https://doi.org/10.1534/g3.111.000240 |
| BWA v.0.7.15 | Heng[74] | http://arxiv.org/abs/1303.3997 |
| SAMtools v1.9 | Heng et al.[75] | https://doi.org/10.1093/bioinformatics/btp352 |
| ADMIXTURE 1.3.0 | Alexander and Novembre[76] | https://doi.org/10.1186/1471-2105-12-246 |
| PLINK v1.9 | Purcell et al.[77] | https://www.sciencedirect.com/science/article/pii/S0002929707613524 |
| STRUCTURE v2.3.4 | Pritchard and Donnelly[78] | https://doi.org/10.1093/genetics/155.2.945 |
| PGDSpider v.2.1.1.5 | Lischer and Excoffier[79] | https://doi.org/10.1093/bioinformatics/btr642 |
| ANGSD v0.923 | Korneliussen et al.[80] | https://doi.org/10.1186/s12859-014-0356-4 |
| Stairway plot v2.1.1 | Liu and Fu[81] | https://doi.org/10.1186/s13059-020-02196-9 |
| R v.4.0.3 | R core team[82] | https://www.R-project.org/ |
| R package, popgenome | Pfeifer et al.[83] | https://cran.r-hub.io/web/packages/PopGenome/index.html |
| R package, hierfstat | Goudet[84] | https://cran.r-project.org/web/packages/hierfstat/index.html |

(*Continued on next page*)

*Continued*

| REAGENT or RESOURCE | SOURCE | IDENTIFIER |
|---|---|---|
| R package, SNPRelate | Zheng et al.[85] | http://bioconductor.org/packages/release/bioc/html/SNPRelate.html |
| R packags, ncf | Bjornstad[86] | https://cran.r-project.org/package=ncf |
| R package, poppr | Kamvar et al.[87] | https://cran.r-project.org/web/packages/poppr/index.html |
| R package, ResDisMapper | Tang et al.[88] | https://github.com/takfung/ResDisMapper |
| R package, ResistanceGA | Peterman[89] | https://github.com/wpeterman/ResistanceGA |
| R package, smatr | Warton[90] | https://cran.r-project.org/web/packages/smatr/index.html |
| Other | | |
| Olympus SZX16 Stereozoom microscope | Olympus | https://www.olympus-lifescience.com/en/microscopes/stereo/szx16/ |

## RESOURCE AVAILABILITY

### Lead contact

Further information and requests for resources should be directed to and will be fulfilled by the lead contact, Yeo Huiqing (huiqing_yeo@u.nus.edu).

### Materials availability

This study did not generate new unique reagents or materials.

### Data and code availability

- Data: All sequences are available on Genbank (PRJNA988429) and metadata is available at: https://data.mendeley.com/datasets/tsf62dsvd4/1.
- Code: All R code and command line code is available at: https://github.com/huiqingyeooo/Ae_albopictus_popgen. Raw Sequences: All raw sequences generated from this study are available on Genbank (BioProject number: PRJNA988429)
- Any additional information required to reanalyze the data reported in this paper is available from the lead contact upon request.

## EXPERIMENTAL MODEL AND STUDY PARTICIPANT DETAILS

### Mosquito samples

Collection of *Ae. albopictus* was carried out in Singapore, one of the most densely populated cities in the world with a population size of 5.4 million residing in a total land area of 719.9 $km^2$. Situated at the southern tip of the Malay Peninsula, the city experiences a tropical rainforest climate with little temperature, rainfall and humidity fluctuations throughout the year.[91] As a result of its small geographical size, land use is highly fragmented with multiple habitat types embedded within an urban matrix. In this study, the sampling habitats of *Ae. albopictus* were broadly grouped into three categories – urban, managed park, and forest (Figure 2A). The habitat categories were defined based on a high resolution surface map of Singapore[92] (Table S3).

Samples were acquired from May 2019 to November 2021 throughout Singapore, including in restricted military areas and on offshore islands – Pulau Tekong and Pulau Ubin (Figure 2A, Document S2). Larvae were collected through opportunistic searching of suitable breeding containers (e.g., flower pots and tree holes). Larvae were also received from the Environmental Health Institute, National Environmental Agency, which were collected as part of the nation-wide residential mosquito surveillance program. Larvae were fed with crushed fish food Tetra® TetraBits and reared individually to the adult stage in an insectary (Department of Biological Sciences, National University of Singapore). Adults were collected from the field by using Centres for Disease Control and Prevention miniature light traps and fan-based aspirators. Trapping sites were at least 50 m apart.[93,94] Some adult samples were collected in military areas (Western Training Area and Pulau Tekong) using Biogents traps by staff of the Singapore Armed Forces.

## METHOD DETAILS

### Identification and storage

All samples were morphologically identified under a stereozoom microscope SZX10 (Olympus, Japan), making sure to look out for characteristics which differentiate *Ae. albopictus* from another sympatric and morphologically similar species, *Ae. malayensis*. A total of 114 *Ae.*

*albopictus* individuals from 91 unique localities were included in the study, 95 of which were larvae, and the remaining 19 were adults. All samples were stored dry at −80°C for subsequent processing.

## Extraction and library preparation

To standardise the amount of starting material and account for damaged specimens with missing appendages, we removed all the legs and wings of each sample, leaving the head, thorax and abdomen for extractions. We extracted genomic DNA from all samples using the DNeasy Blood & Tissue Kit (Qiagen, Germany) following the manufacturer's protocol. Double-digest restriction enzyme-associated sequencing libraries (ddRADSeq) were prepared as described elsewhere.[95,96] Briefly, 400 ng of genomic DNA from each sample was digested with 20 units of EcoRI and 4.4 units of MspI in a 50 μl reaction with NEB CutSmart buffer and water (New England Biolabs, Beverly MA, USA). Digestions were carried out at 37.5°C for 3.5 hours with no heat kill step, and the digested products were cleaned with Ampure XP paramagnetic beads (Beckman Coulter, Brea, CA). They were ligated to P1 and P2 adapters with T4 ligase (New England Biolabs, Beverly MA, USA) for 16 hours at 16°C, followed by 65°C for 20 minutes, and thereafter a stepwise decrease in temperature of 1°C per minute to 23°C.

We carried out size selection using a Pippin Prep 2% gel cassette (Sage Sciences, Beverly, MA), retaining DNA fragments of 305 to 365 bp, which were cleaned with Ampure XP beads. Four libraries were created by pooling 26-29 samples into each library. Each library was enriched by a 12-cycle PCR in 50 μl reactions containing 15 μl of cleaned library DNA, 10 μl of Q5 reaction buffer, 1 μl of 10 nM dNTPs, 1.5 μl of Illumina P1 and P2 primers, 1 μl of Q5 Hotstart HF DNA polymerase and 20 μl of molecular-grade RNase-free water. PCR products were cleaned up with Ampure XP beads. Sample library fragment size distributions were obtained using a Fragment Analyzer (Advanced Analytical Technologies, Ankeny, IA, USA). Final library concentrations were measured with a Qubit® 2.0 Fluorometer (Thermo Fisher Scientific) before pooling with unrelated samples in equimolar volumes. Sequencing was carried out on an Illumina NovaSeq 6000 S4 flow cell using 150 bp paired-end chemistry (Macrogen APAC, Seoul, South Korea).

## Demultiplexing, filtering and SNP calling

Adapter sequences were removed with Cutadapt[71] and sequence quality was analysed with FastQC (Babraham Bioinformatics, USA). We retained all sequences with phred scores ≥20 without truncation. Demultiplexing and clean up were carried out with the program process_radtags as implemented in Stacks v2.41[73,97] with the quality filters -q and -c to discard reads with phred scores <20 and to remove reads with uncalled bases, respectively. In total 2.501 billion reads across all four libraries, averaging 22.133 million reads per individual (median: 23,790,498; range: 194,237–40,143,269) were retained for further filtering (Figure S7).

We carried out repeat masking to the most complete *Ae. albopictus* reference genome.[98] Reads were aligned using BWA-MEM as implemented in BWA v.0.7.15.[74] Aligned reads with a minimum MAPQ score of 20 were retained and sorted into coordinate order with SAMtools v1.9.[75] We used the pipeline ref_map.pl in Stacks to call single nucleotide polymorphic markers (SNPs) without prior population assignment.

We first explored multiple SNP calling regimes using Populations in Stacks v1.34, allowing for 10%, 20% and 25% missing data across loci as well as a minimum minor allele frequency (MAF) of 0, 0.01, 0.03 and 0.05. Sensitivity analyses were conducted by computing summary statistics with the R packages popgenome and hierfstat,[83,84] carrying out principal component analysis (PCA) (Figure S8) and ADMIXTURE 1.3.0[76,99] (Figure S9). The results of sensitivity analyses were not different across datasets with varying percentages of missing data (Figures S8 and S9). However, a decreasing stringency of MAF resulted in weaker population structure as more of the rarer alleles were included, thereby diluting population signal.[100] Taking these considerations into account, we decided on two separate datasets: dataset 1) allowing for 0.05 MAF for population structure and ancestry inference (PCA and STRUCTURE), and dataset 2) with 0 MAF for the rest of the analyses.

To reduce the effects of linkage disequilibrium in subsequent analyses, all pairwise SNPs with squared correlation ($r^2$) greater than 0.9 within a 25 kbp window frame sliding 10 bp at a time were pruned using PLINK v1.9.[77,101] Using the same software, six individuals that had less than 3X coverage across loci or more than 20% missing data across loci were removed before calling SNPs again. The final datasets had a mean coverage of 17.3X (median: 18.3X) across loci from 107 individuals, ranging from 2,349,038 – 40,143,269 reads with an average of 23,022,078 reads and a median of 24,430,385 reads. Dataset 1 consisted of 27,037 SNPs and dataset 2 had 35,101 SNPs.

## Quantitative PCR

We carried out quantitative PCR on a subset of 90 *Ae. albopictus* samples. As most of the samples used for estimating *Wolbachia* infection loads were adult females (94.8%), we did not exclude the remaining few individuals (males and larvae: 5.2%) from the dataset as it did not significantly affect the analysis. We refrained from analyzing *Wolbachia* density by sex and age of the mosquitoes because of the rarity of males in our dataset and a lack of information about the age of wild-caught individuals which made up a substantial proportion of our dataset.

We utilised two primer sets to quantify *Wolbachia* density from two supergroups – *w*AlbA and *w*AlbB (Table S4).[70] To make comparisons across *Ae. albopictus* samples, the single copy ribosomal S7 gene was also quantified to allow for normalisation of *Wolbachia* density.[41] Quantitative PCR was carried out in 10 μl reactions, containing 5 μl of SsoAdvanced™ Universal SYBR® Green Supermix (Bio-Rad, California, USA), 1 μl each of 5 μM forward and reverse primers, 2 μl of molecular water and 1 μl of extracted DNA. We employed the following protocol: 98°C for 3 minutes, followed by 35 cycles of 98°C for 15 seconds, annealing temperature for 15 seconds, and 72°C for 15 seconds in a C1000 Touch™ Thermal Cycler (Bio-Rad). The PCR protocol was optimised by checking the melting curve profiles and primer efficiencies for each gene before proceeding with all the samples. Each sample was amplified twice as duplicates.[39] DNA from *Wolbachia*-infected *Ae. albopictus* was used as a positive control and molecular-grade water was used as a negative control.

## QUANTIFICATION AND STATISTICAL ANALYSIS

### Population genomic approaches

We conducted file format conversions necessary for all subsequent analyses with PGDSpider v2.1.1.5.[79] All analyses with R packages were performed in R 4.0.3.[82] Heterozygosity estimates were calculated with the R package hierfstat using dataset 2, ensuring that low-coverage sites (<3x) were removed, filtering for <25% missingness and ensuring that minor allele frequency cutoffs were not implemented.[102,103] Pairwise relatedness was estimated across all individual pairs using a maximum likelihood algorithm[104,105] as implemented in the R package SNPRelate.[85] Two pairs of individuals (APG41 and APG87, r = 0.259; APG48 and APG73, r = 0.233) were determined to be closely related kin (r > 25%). As related individuals may affect downstream analyses, the individual with the lower coverage from each related pair was removed. To visualise potential population structure among the remaining 105 individuals, we carried out PCA as implemented in SNPRelate. A partial Mantel test was then carried out to test for IBD while accounting for pairwise leaf area index using the package ncf.[86] The genetic distance matrix was generated with prevosti.dist as implemented in poppr.[87]

To explore population structure within *Ae. albopictus* across Singapore, we ran STRUCTURE v2.3.4[78] as implemented in Structure_threader.[106] We tested one to eleven population subdivisions (K) with 10 runs for each K value tested; for each run, we discarded the first 100,000 generations as burnin and measured the posterior with the following 500,000 generations of Markov Chain Monte Carlo (MCMC). To determine the most likely K value of population subdivisions, we evaluated Delta K[107] using StructureHarvester v0.6.94.[108] Clumpp v1.1.2[109] was used to integrate and summarise runs from output files of the best K. The optimal number of K-clusters in STRUCTURE was determined to be K = 2 using the Evanno method.[107]

To examine the recent demographic history of *Ae. albopictus* in Singapore, a folded site frequency spectrum (SFS) was generated using ANGSD v0.923 with the SAMtools genotype likelihood method and ANGSD function realSFS. Historical population size changes were then estimated assuming a mutation rate of $2.8 \times 10^{-9}$ site$^{-1}$ generation$^{-1}$ [110] and a generation time of 0.0384 years[62,111,112] using Stairway plot v2.1.1.[81]

### Landscape genetic optimisation

We further examined dispersal of *Ae. albopictus* in Singapore using a spatially explicit, individual-based approach implemented in the R package ResDisMapper.[88] This method is suitable for mapping resistance to ongoing dispersal within a geographically continuous population at small spatiotemporal scales. Distributions of genetic distance (Prevosti's distance) and geographic distance were checked using linear and non-linear modelling methods. The linear model was determined to be the best-fit model. We then calculated resistance values and their corresponding statistical significance using 5 km, 10 km, and 20 km as maximum distance. The resistance values were visualized as raster layers with two separate colours depicting lower and higher than expected gene flow respectively, and cells without statistical certainty were masked in white.

To assess the effects of landscape features on gene flow in *Ae. albopictus*, we utilised a circuit theory resistance method implemented in ResistanceGA.[89] ResistanceGA is a novel approach to transform and optimise resistance surfaces to optimally fit genetic data while accounting for spatial autocorrelation.[89] After pairwise genetic distances were calculated, Circuitscape[113] was run to calculate pairwise resistance distances between individuals using their coordinates and employ a genetic algorithm to maximize fit of resistance values to the environmental surfaces. Linear mixed effects models were fitted using the maximum likelihood population effects parameterization.[114] We used AICc[115] as our objective criterion for optimization. A distance model was included to account for IBD, and a null model was also included for comparison.

A total of seven environmental surfaces were obtained from published sources and were tested (Figure S3). Categorical surfaces include land use[116] and land surface type.[92] As the land surface raster consisted of 13 categorical landscape features, we also explored merging some of the relevant categories to create a raster layer with five categories (Figure S3). Feature surfaces included location of dengue clusters in 2021,[117] location of dengue cases in 2018,[118] and areas with a high *Ae. aegypti* population from April to June 2019.[119] We also included the leaf area index,[120] which is a continuous surface, and employed monomolecular functions to transform continuous resistance surfaces.[89] All raster surfaces had a cell size of 200 × 200 m. ResistanceGA was run five times for each model,[89] and checked for convergence. Results from the best model among all replicates were used.

Although both land surface and reclassified land surface raster layers had lower AICc values than the distance model (Figure S4A), the variation in resistance values for the reclassified land surface layer was greater than the land surface layer (Figure S4B). Among the 13 categories of the land surface layer, resistance values in five were observed to be largely consistent across replicates (buildings, open greenery, forest, marine and artificial impervious) (Figure S4C). Hence, we used results of these five categories from the land surface raster layer to interpret the analysis.

We were additionally curious to explore if the distributions and infection densities of *Wolbachia* wAlbA and wAlbB could be optimised as explanatory variables for *Ae. albopictus* gene flow using various estimates of kernel density (Figure S10). As these layers were only generated from individual points where *Ae. albopictus* individuals were collected for this study, and do not account for false absence of *Wolbachia*-infected individuals in non-sampled areas, we decided not to incorporate the results into our study but present them as supplementary results. The results may be informative for researchers who wish to explore the use of biotic factors as explanatory variables in landscape genetic analyses.

### *Wolbachia* density analyses

Our criterion for the inclusion of a sample in subsequent statistical analyses was that the difference between replicate Cq values must be less than 0.5 across all genes.[41] By applying a strict but reliable criterion, we excluded 14 out of 91 (15.4%) of our samples. The final dataset consisted of 77 samples: 26 from forested areas, 15 from managed parkland and 36 from urban areas. We calculated relative *Wolbachia* densities using the following formula:

$$Wolbachia\ density\ =\ 2^{Cq(RpS7)\ -\ Cq(wAlbA/Bq\ -\ wsp)}$$

All *Wolbachia* density values were log10-transformed to normalize the distribution and reduce heteroscedasticity (Packard et al., 2011) prior to analysis. As we were interested in investigating the relationship between *w*AlbA and *w*AlbB densities, as opposed to predicting *Wolbachia* infection loads, we carried out correlations with standardised major axis (SMA) analysis instead of linear regression models. We used the R package smatr[90] to determine the best-fitting lines for the relationship between *w*AlbA and *w*AlbB and tested for differences in slope and elevation of the best fit lines across the three habitat categories.